


 CrossMark
click for updates

 Cite this: *CrystEngComm*, 2015, 17, 3533

The structure of monoclinic Na₂B₁₀H₁₀: a combined diffraction, spectroscopy, and theoretical approach†

 Hui Wu,^{*ab} Wan Si Tang,^{ab} Wei Zhou,^{ab} Vitalie Stavila,^c John J. Rush^{ab} and Terrence J. Udovic^{*a}

Neutron powder diffraction measurements of a specially synthesized Na₂¹¹B₁₀D₁₀ compound, buttressed by comparative measurements and calculations of vibrational dynamics, have led to an improved, Rietveld-refined, structural model for its low-temperature monoclinic phase. The detailed atomic arrangements and phases for this compound are important for an understanding of its potential roles for fast-ion-battery and hydrogen-storage applications. A comparison of the calculated phonon densities of states (PDOSs) based on density functional theory for both the previously published structure and our new modified structure show that the PDOS of the latter is in noticeably better agreement with that experimentally observed by neutron vibrational spectroscopy. Moreover, this improved structure is predicted to have a higher stability and exhibits more reasonable separations between all neighboring sodium cations and decahydro-*closo*-decaborate anions. These results demonstrate the effectiveness of combining first-principles computational methods and neutron-based structural and spectroscopic techniques for determining crystal structures for such complex hydrogenous materials.

 Received 20th February 2015,
Accepted 7th April 2015

DOI: 10.1039/c5ce00369e

www.rsc.org/crystengcomm

Introduction

Sodium decahydro-*closo*-decaborate (Na₂B₁₀H₁₀), an ionic compound comprised of decahedral B₁₀H₁₀²⁻ anions and Na⁺ cations, has gained sudden technological relevance by the recent discovery that its phase transition from an ordered monoclinic structure to a disordered face-centered-cubic (fcc) structure near 370 K to 380 K is accompanied by the appearance of exceptional Na⁺ superionic conductivity (≈ 0.01 S cm⁻¹ at 383 K).¹ This order–disorder transition temperature is around 150 K lower than that for the related compound, Na₂B₁₂H₁₂.^{2–4} The lower transition temperature, high conductivity, and favorable electrochemical stability¹ makes

Na₂B₁₀H₁₀ a compelling candidate electrolyte material for use in next-generation, solid-state rechargeable Na-ion batteries,^{5,6} in both its current and potential chemically modified forms. Moreover, Na₂B₁₀H₁₀ has relevance as a possible by-product to be considered during the dehydrogenation of NaBH₄, a lightweight borohydride that is being investigated as a potential hydrogen-storage material.^{7,8}

A fundamental understanding of this compound's thermodynamic properties and temperature-dependent structural behavior as well as meaningful computational studies geared toward further improvements in its properties requires accurate structural information. Due to the inability to easily synthesize single crystals of solvent-free alkali-metal decahydro-*closo*-decaborates, Hofmann and Albert⁹ reported monoclinic *P*2₁/*n*-symmetric crystal structures for polycrystalline Na₂B₁₀H₁₀ and K and Rb congeners based on X-ray powder diffraction (XRPD) data in conjunction with direct-space, simulated-annealing, powder techniques. Although their Na₂B₁₀H₁₀ monoclinic structure was in reasonable agreement with the measured XRPD pattern, a preliminary analysis of our neutron powder diffraction (NPD) patterns for Na₂¹¹B₁₀D₁₀ indicated inconsistencies with this structure. The authors themselves suggested that their structure may lack precision with regard to boron atom positions.⁹ In addition, a closer scrutiny of this structure revealed the presence of some unusual Na–H distances of around 1.6 Å, which are much shorter than expected when compared with the

^a NIST Center for Neutron Research, National Institute of Standards and Technology, Gaithersburg, MD 20899–6102, USA. E-mail: hui.wu@nist.gov, udovic@nist.gov

^b Department of Materials Science and Engineering, University of Maryland, College Park, MD 20742–2115, USA

^c Energy Nanomaterials, Sandia National Laboratories, Livermore, CA 94551, USA

† Electronic supplementary information (ESI) available: Simulated NPD patterns for the modified and published monoclinic structures. NPD and XRPD patterns and structure tables of the high-temperature disordered cubic structure. Plots of the lattice parameters *versus* temperature for the modified structure. Comparison of the unit cells for the published structure before and after energy-optimization. Structure tables and CIF files for NPD-refined and XRPD-refined modified structures. Tables of DFT-generated phonon symmetries and energies. Instructions and datafiles to generate animations of all vibrational modes contributing to the simulated PDOSs of the modified structure. See DOI: 10.1039/c5ce00369e.

minimum Na–H distances of greater than 2.2 Å associated with the structurally related monoclinic Na₂B₁₂H₁₂.¹⁰

These observations suggested that an improved monoclinic Na₂B₁₀H₁₀ structure existed. In this paper, we report such a structure, solved *via* Rietveld refinement using NPD data and guided by both direct-space, simulated-annealing and DFT energy-optimization methods, and comparisons between calculated and observed neutron vibrational spectra. For additional comparison, complementary synchrotron XRPD measurements are also analyzed. This study illustrates the importance of using a combination of techniques, both experimental and theoretical, for determining the most physically reasonable structure associated with a complex hydrogenous material.

Experimental details

Since ¹⁰B comprises 20% of natural boron and is a strong neutron absorber, we produced ¹¹B-enriched materials for all neutron scattering measurements. For NVS measurements, Na₂¹¹B₁₀H₁₀ was synthesized by first forming (H₃O)₂¹¹B₁₀H₁₀ from ¹¹B₁₀H₁₄ (Katchem¹¹) and triethylamine,¹ neutralizing the (H₃O)₂¹¹B₁₀H₁₀ with 0.1 M NaOH to a pH of 7, and drying the resulting aqueous Na₂¹¹B₁₀H₁₀ first with a rotary evaporator at 323 K to form a solid hydrate followed by complete dehydration under vacuum at 433 K for 16 h. Natural-boron-containing Na₂B₁₀H₁₀ for XRPD measurements was synthesized in a similar fashion starting with B₁₀H₁₄ (Sigma-Aldrich). Some of the Na₂¹¹B₁₀H₁₀ material was fully deuterated (>99%) to Na₂¹¹B₁₀D₁₀ for both NPD and additional neutron vibrational spectroscopy (NVS) measurements using four sequential exchange treatments in DCl-acidified D₂O, based on the work of Muetterties *et al.*¹² and further described elsewhere.¹³ Complete D–H exchange was confirmed by model refinement of the NPD pattern for the anhydrous product at 2.5 K.

Neutron scattering measurements were performed at the National Institute of Standards and Technology Center for Neutron Research. NPD patterns for Na₂¹¹B₁₀D₁₀ were measured on the BT-1 High-Resolution Powder Diffractometer¹⁴ at 2.5 K, 295 K, and 410 K using the Cu(311) monochromator ($\lambda = 1.5398(2)$ Å). Horizontal divergences of 60', 20', and 7' of arc were used for the in-pile, monochromatic-beam, and diffracted-beam collimators, respectively. The sample was contained in a 6 mm diameter V can inside a He closed-cycle refrigerator. NVS measurements of both Na₂¹¹B₁₀H₁₀ and Na₂¹¹B₁₀D₁₀ at 4 K were performed on the Filter-Analyzer Neutron Spectrometer (FANS)¹⁵ using the Cu(220) monochromator with pre- and post-collimations of 20' of arc, yielding a full-width-at-half-maximum energy resolution of about 3% of the neutron energy transfer. XRPD patterns of Na₂B₁₀H₁₀ were measured between 100 K and 410 K at the Advanced Photon Source on Beamline 17-BM-B at Argonne National Laboratory using a Si(111) monochromator ($\lambda = 0.7296(1)$ Å).

To assist the structural refinements, first-principles calculations were performed within the plane-wave implementation

of the generalized gradient approximation to Density Functional Theory (DFT) using a Vanderbilt-type ultrasoft potential with Perdew–Burke–Ernzerhof exchange.¹⁶ A cutoff energy of 544 eV and a $2 \times 2 \times 1$ *k*-point mesh (generated using the Monkhorst-Pack scheme) were used and found to be enough for the total energy to converge within 0.01 meV per atom. For comparison with the NVS measurements for Na₂¹¹B₁₀H₁₀ and Na₂¹¹B₁₀D₁₀, simulated phonon densities of states (PDOSs) were generated from DFT-optimized structures using the supercell method ($2 \times 2 \times 1$ cell size) with finite displacements,^{17,18} and were appropriately weighted to take into account the H, D, Na, and ¹¹B total neutron scattering cross sections. In addition, simulated PDOSs of the “isolated” ¹¹B₁₀H₁₀²⁻ and ¹¹B₁₀D₁₀²⁻ anions were generated for comparison using $20 \times 20 \times 20$ supercells and considering their *D*_{4d} molecular symmetries in the phonon calculations.

Some structural depictions were made using the VESTA (Visualization for Electronic and Structural Analysis) software.¹⁹ For all figures, standard uncertainties are commensurate with the observed scatter in the data, if not explicitly designated by vertical error bars.

Results and discussion

Initial attempts to reconcile the NPD data with the published structure were unsuccessful, leading us to search for an alternative structure. The 2.5 K NPD pattern of Na₂¹¹B₁₀D₁₀ was indexed to a monoclinic structure with approximate lattice parameters of $a = 6.672$ Å, $b = 12.979$ Å, $c = 11.868$ Å, and $\beta = 120.23^\circ$. Assessment of the extinction symbol associated with the space group of the low-temperature phase indicated the most probable to be *P*₂₁/*c* (no. 14), as previously determined by Hofmann and Albert.⁹ The crystal structure was solved using direct space methods under this space group. A first-principles DFT calculation was then performed to optimize the ¹¹B₁₀D₁₀²⁻ configuration, particularly the D positions. Rietveld refinement²⁰ of the DFT-relaxed structural model was performed using the GSAS package²¹ on the NPD data. The ¹¹B₁₀D₁₀²⁻ anion was kept as a rigid body due to the large number of variables (22 independent atoms with 66 independent atomic coordinates in one unit cell). The thermal factors of like atoms were constrained to be identical. The ¹¹B₁₀D₁₀²⁻ rigid body together with Na atom coordinates, thermal factors, and lattice parameters were refined, yielding the agreement factors of $R_{wp} = 0.0391$, $R_p = 0.0311$, and $\chi^2 = 1.308$, and lattice parameters of $a = 6.6535(5)$ Å, $b = 12.964(1)$ Å, $c = 11.8510(9)$ Å, and $\beta = 120.203(4)^\circ$.

The 295 K NPD pattern could also be fit using the same model with agreement factors of $R_{wp} = 0.0373$, $R_p = 0.0306$, and $\chi^2 = 1.193$, and lattice parameters of $a = 6.7137(7)$ Å, $b = 13.124(1)$ Å, $c = 11.940(1)$ Å, and $\beta = 120.524(6)^\circ$. The Rietveld fits to the 2.5 K and 295 K NPD patterns are shown in Fig. 1. Refinement parameters are summarized in Tables S1 and S2, and more crystallographic details can be found in the CIF

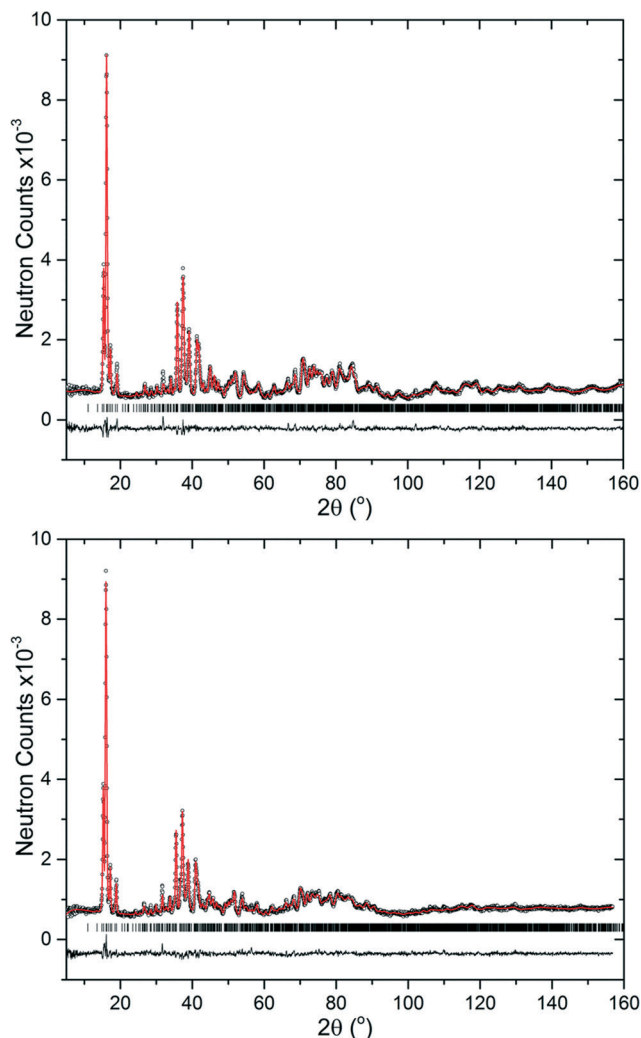


Fig. 1 Experimental (circles), fitted (line), and difference (line below observed and calculated patterns) NPD profiles ($\lambda = 1.5398(2)$ Å) for $\text{Na}_2^{11}\text{B}_{10}\text{D}_{10}$ at 2.5 K (top, $R_{\text{wp}} = 0.0391$, $R_{\text{p}} = 0.0311$, $\chi^2 = 1.308$) and 295 K (bottom, $R_{\text{wp}} = 0.0373$, $R_{\text{p}} = 0.0306$, $\chi^2 = 1.193$). Vertical bars indicate the calculated positions of Bragg peaks.

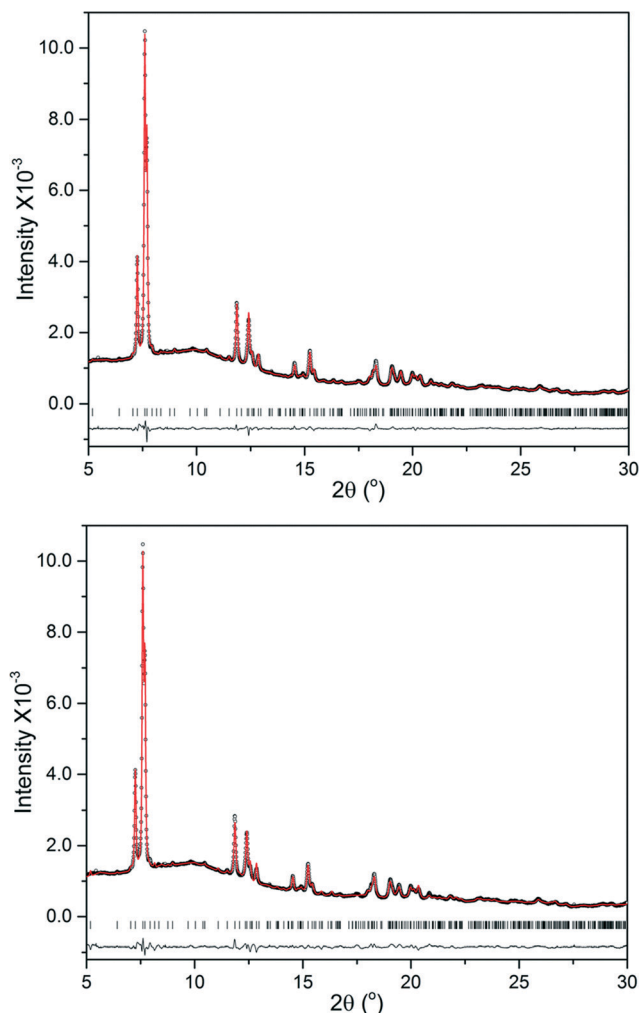


Fig. 2 Experimental (circles), fitted (line), and difference (line below observed and calculated patterns) synchrotron XRPD profiles ($\lambda = 0.7296(1)$ Å) for $\text{Na}_2\text{B}_{10}\text{H}_{10}$ at 100 K refined using the modified crystal structure (top, $R_{\text{wp}} = 0.0765$, $R_{\text{p}} = 0.0854$, $\chi^2 = 0.416$) and the published structure (bottom, $R_{\text{wp}} = 0.111$, $R_{\text{p}} = 0.129$, $\chi^2 = 0.850$). Vertical bars indicate the calculated positions of Bragg peaks.

files in the ESI.† Moreover, Fig. S1 in the ESI† compares the simulated NPD patterns for $\text{Na}_2^{11}\text{B}_{10}\text{D}_{10}$ associated with both the published and modified structures, clearly indicating the broad disagreement between the two structures and confirming the substantial sensitivity of NPD to the particular structural details.

Fig. 2 shows the $\text{Na}_2\text{B}_{10}\text{H}_{10}$ synchrotron XRPD pattern at 100 K and model refinements based on both the published and the NPD-derived structures. Although the differences are minor, the modified structure resulted in a better model fit than the published structure. The ESI contains XRPD refinement parameters and more crystallographic details for the modified structure at both 100 K and 300 K in Tables S3 and S4 and the accompanying CIF files, along with plots of the lattice parameters *versus* temperature in Fig. S2.† Compared to the NPD data, it is clear that the XRPD data are much less sensitive to the orientation and shape of the anions

associated with a particular structural model. In light of the subtle differences observed in Fig. 2, the less accurate results obtained in the original XRPD study⁹ are understandable given the generally greater sensitivity of NPD when used to refine the detailed structure of a complex hydrogenous material.

For completeness, in addition to the monoclinic structure, the ESI contains the refinement parameters and crystallographic details (Fig. S3 and Tables S5 and S6†) for the high-temperature cubic structure¹ at 410 K based on both $\text{Na}_2^{11}\text{B}_{10}\text{D}_{10}$ NPD and $\text{Na}_2\text{B}_{10}\text{H}_{10}$ synchrotron XRPD data.

Fig. 3 compares the unit cells of the modified and published structures. As expected, the two monoclinic structures are rather similar with respect to the relative Na^+ cation and $\text{B}_{10}\text{H}_{10}^{2-}$ anion positions. The main differences lie in the relative orientations and distortions of the anions, the anions deviating more from their ideal D_{4d} -symmetric shape in the

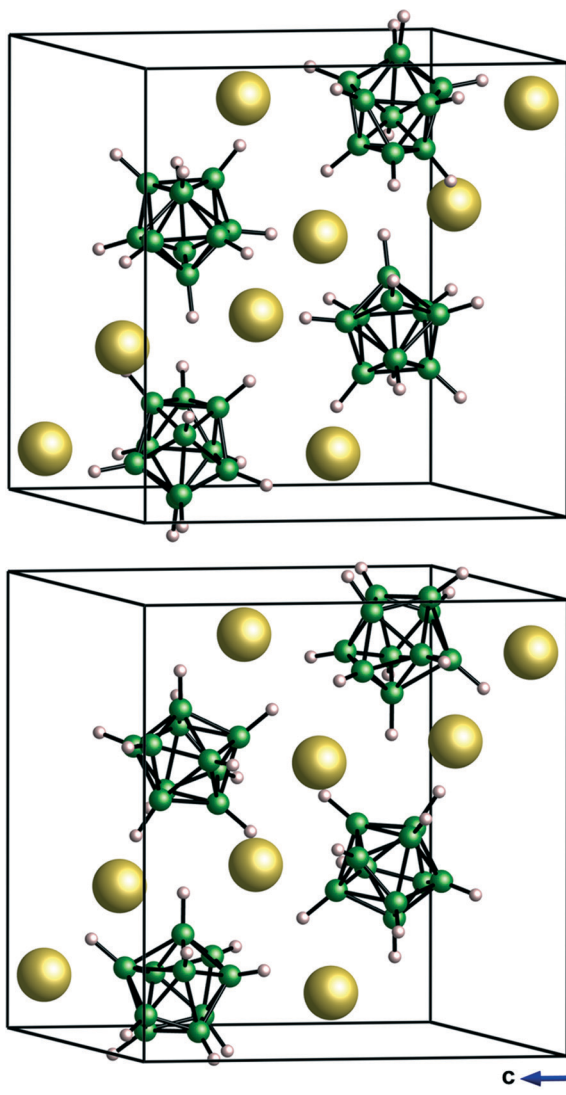


Fig. 3 The modified monoclinic $\text{Na}_2^{11}\text{B}_{10}\text{D}_{10}$ crystal structure (top) compared to the published structure⁹ (bottom). Yellow, green, and white spheres denote Na, B, and D atoms, respectively.

published structure. This is in line with the previous authors' caution that their XRPD-derived structure may lack precision with regard to boron (and hydrogen) atom positions.⁹

Fig. 4 depicts the corresponding eightfold Na^+ cation coordinations around each anion as well as the cation–anion distances in the modified 2.5 K $\text{Na}_2^{11}\text{B}_{10}\text{D}_{10}$ and published 100 K $\text{Na}_2\text{B}_{10}\text{H}_{10}$ structures. For the modified structure, the distances between the Na^+ cations and the center of the anion (at 2.5 K) vary from 3.979 Å to 4.471 Å, similar in range to that of the published $\text{Na}_2\text{B}_{10}\text{H}_{10}$ structure (at 100 K).

Fig. 5 illustrates the irregular tetrahedral coordination of anions surrounding each of the two crystallographically distinct Na cations in the Na1 and Na2 sites of the modified structure. The distances (at 2.5 K) between Na and the nearest D atoms vary from 2.151 Å to 2.788 Å. The minimum Na–D distance observed is in line with that observed in monoclinic $\text{Na}_2^{11}\text{B}_{12}\text{D}_{12}$ (2.251 Å at 7 K).²

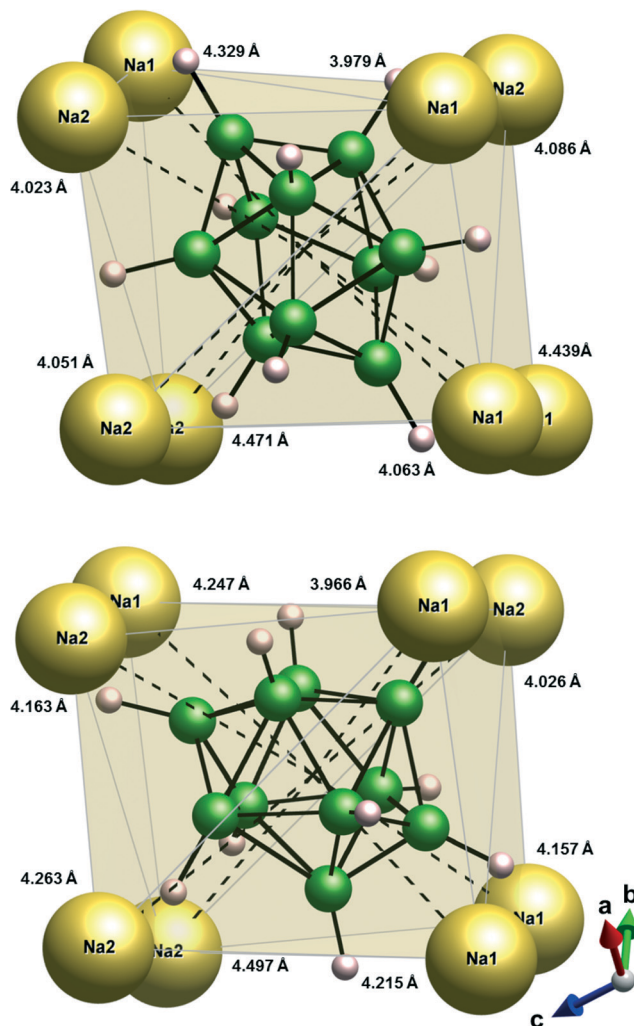


Fig. 4 The Na^+ cation coordination around each anion associated with the (top, 2.5 K) modified $\text{Na}_2^{11}\text{B}_{10}\text{D}_{10}$ and (bottom, 100 K) published⁹ $\text{Na}_2\text{B}_{10}\text{H}_{10}$ structures. The distances between the Na^+ cations and the centers of the anions are indicated.

Fig. 6 and 7 compare the relative orientations of $\text{B}_{10}\text{H}_{10}^{2-}$ anions with respect to the Na1 and Na2 sites in the modified $\text{Na}_2\text{B}_{10}\text{H}_{10}$ structure to those in the published structure. In the modified structure, Na1 is in closest proximity to a B–B edge (and their associated H atoms) from each of three neighboring $\text{B}_{10}\text{H}_{10}^{2-}$ anions and to a trigonal face from the remaining neighboring $\text{B}_{10}\text{H}_{10}^{2-}$ anion; Na2 is in closest proximity to a B–B edge from each of two neighboring $\text{B}_{10}\text{H}_{10}^{2-}$ anions and to a trigonal face from each of the remaining two neighboring $\text{B}_{10}\text{H}_{10}^{2-}$ anions. In the published structure, Na1 is in closest proximity to a trigonal face from each of the four neighboring $\text{B}_{10}\text{H}_{10}^{2-}$ anions; Na2 is in closest proximity to a trigonal face from each of two neighboring $\text{B}_{10}\text{H}_{10}^{2-}$ anions and to a vertex from each of the remaining two neighboring $\text{B}_{10}\text{H}_{10}^{2-}$ anions. The unusual orientations for the latter two anions yield abnormally and nominally short Na–H distances of 1.605 Å and 2.034 Å, respectively, at 100 K. The shorter distance is on the order of 0.5 Å smaller than expected,

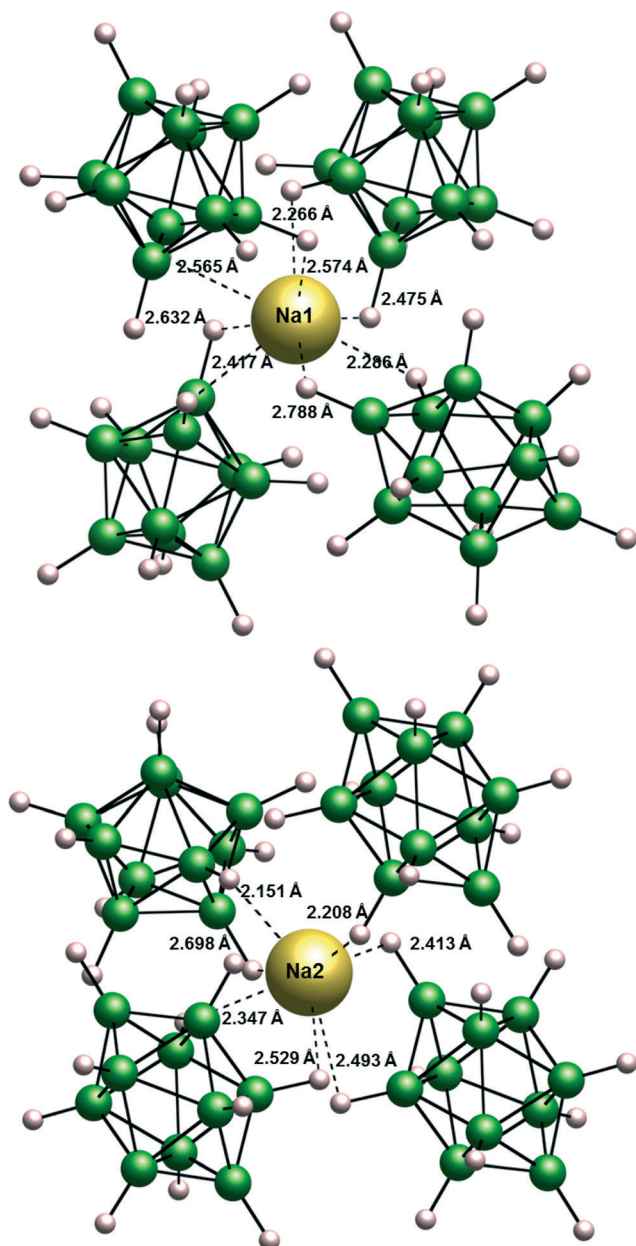


Fig. 5 Tetrahedral coordinations of the two crystallographically distinct Na cations in the modified $\text{Na}_2^{11}\text{B}_{10}\text{D}_{10}$ monoclinic structure. The distances (at 2.5 K) between Na and the nearest D atoms are indicated.

based on the minimum Na–D distances observed in the modified $\text{Na}_2^{11}\text{B}_{10}\text{D}_{10}$ structure and the related $\text{Na}_2^{11}\text{B}_{12}\text{D}_{12}$ compound.²

The calculated energy at 0 K of the modified monoclinic structure is found to be lower than that of the published structure by ≈ 550 meV per unit cell, based on a $\text{Na}_8(\text{B}_{10}\text{H}_{10})_4$ unit cell with 88 atoms. The difference, although not large, is significantly higher than the uncertainty of the calculation, which is typically < 0.1 meV per atom. Hence, the calculation suggests that the modified structure is indeed more stable than the published structure, after energy-optimization of each. It should be noted that the modified structure was little

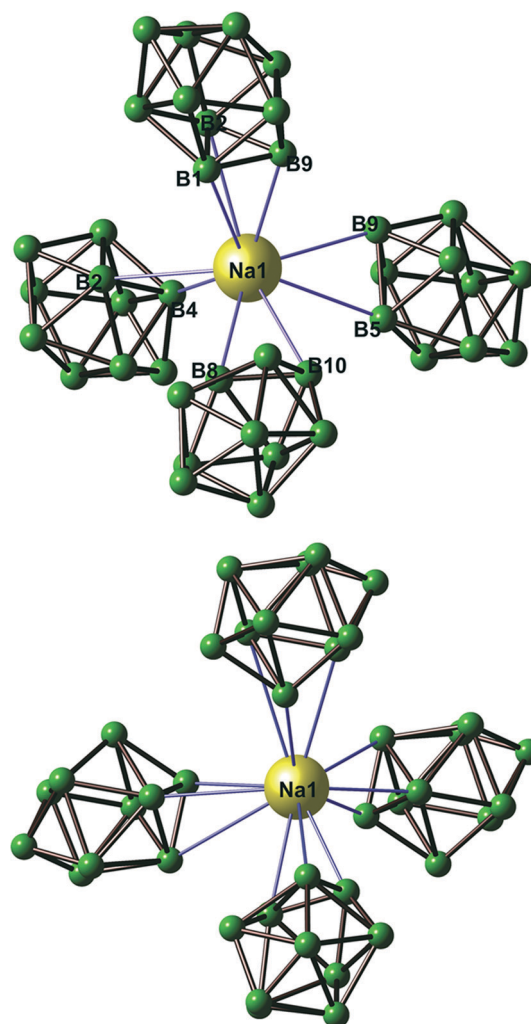


Fig. 6 The relative orientations of $\text{B}_{10}\text{H}_{10}^{2-}$ anions (with H atoms omitted for clarity) with respect to Na1 in the modified $\text{Na}_2\text{B}_{10}\text{H}_{10}$ structure (top) compared with those in the published structure⁹ (bottom).

changed by energy-optimization, further corroborating its authenticity, unlike the published structure, which underwent much more noticeable alteration. The comparison of the published structure before and after energy-optimization is shown in Fig. S4 in the ESI.†

The neutron vibrational spectra for $\text{Na}_2^{11}\text{B}_{10}\text{H}_{10}$ and $\text{Na}_2^{11}\text{B}_{10}\text{D}_{10}$ at 4 K are shown in Fig. 8a and 9a, respectively. They are compared with the simulated PDOSs based on the DFT-optimized versions of the modified structure (Fig. 8b and 9b), the published structure (Fig. 8c and 9c), and “isolated” $^{11}\text{B}_{10}\text{H}_{10}^{2-}$ and $^{11}\text{B}_{10}\text{D}_{10}^{2-}$ anions (Fig. 8d and 9d). The PDOSs of the isolated anions demonstrate the vibrational behavior of anions that are unperturbed by the close-packed structural arrangement of cations and anions.

Due to the relatively large neutron scattering cross-section for H atoms compared to Na or ^{11}B atoms, the $\text{Na}_2^{11}\text{B}_{10}\text{H}_{10}$ spectrum is dominated by the optical vibrational modes involving H-atom displacements. The somewhat lower scattering cross-section for D atoms means that the $\text{Na}_2^{11}\text{B}_{10}\text{D}_{10}$

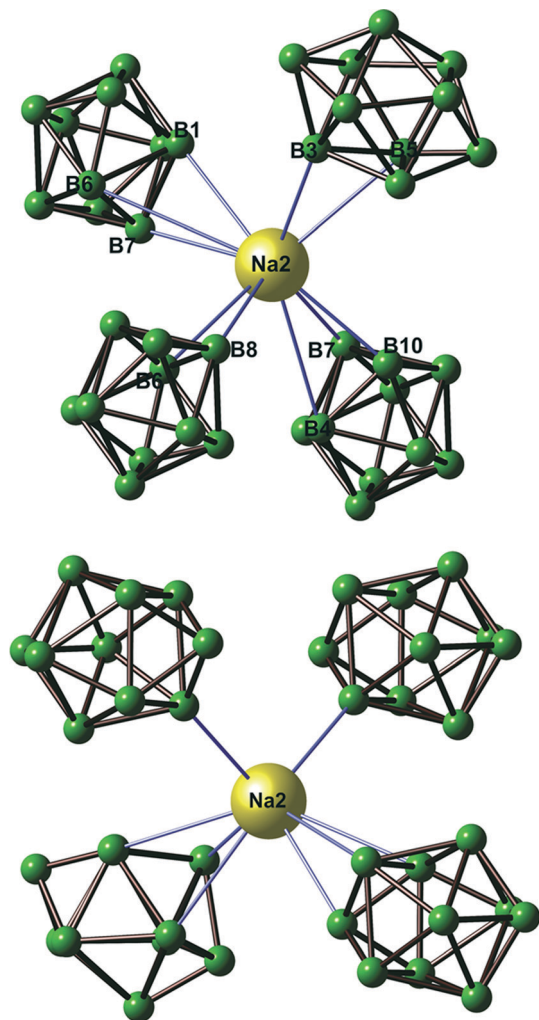


Fig. 7 The relative orientations of $B_{10}H_{10}^{2-}$ anions (with H atoms omitted for clarity) with respect to Na2 in the modified $Na_2B_{10}H_{10}$ structure (top) compared with those in the published structure⁹ (bottom).

spectrum has relatively more scattering contributions from the Na and ^{11}B atom displacements.

Previous studies of $B_{12}H_{12}^{2-}$ -anion-based compounds²² has shown a clear sensitivity of the observed PDOSs to the variety of crystal structure arrangements, with DFT-generated PDOSs clearly corroborating the diffraction-derived structures. A more recent structural study of $Li_2B_{10}H_{10}$ has also indicated that the corresponding DFT-generated PDOS accurately reproduces the fine details of the observed neutron vibrational spectrum.¹³ This suggests that DFT accurately describes both the intramolecular and intermolecular bonding potentials for both dodecahydro-*closo*-dodecaborate and decahydro-*closo*-decaborate ionic compounds. Hence, it is reasonable to expect that, if the structural model is correct, there should be good agreement between the DFT-generated and experimental PDOSs for $Na_2B_{10}H_{10}$ and $Na_2B_{10}D_{10}$.

The $Na_2^{11}B_{10}H_{10}$ spectral results shown in Fig. 8 indicate much better overall agreement between experiment and theory for the modified structure compared to that for the

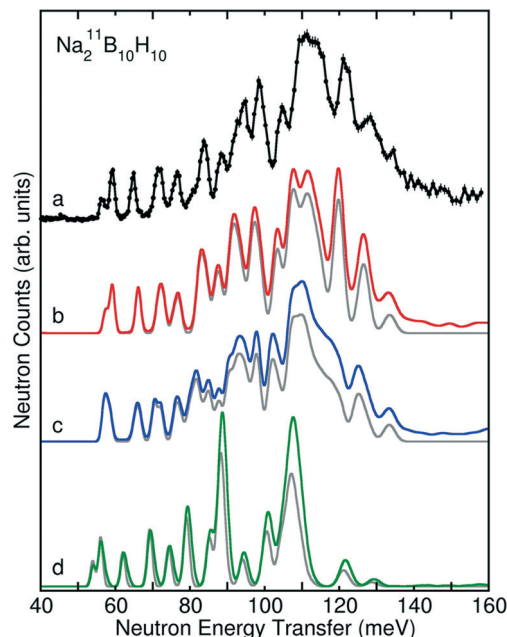


Fig. 8 Neutron vibrational spectrum (a) of $Na_2^{11}B_{10}H_{10}$ at 4 K compared to the simulated one-phonon (gray) and one + two-phonon densities of states (red, blue, and green) from first-principles phonon calculations of the different DFT-optimized structures: (b) current NPD-refined modified structure, (c) published structure,⁹ and (d) "isolated" $^{11}B_{10}H_{10}^{2-}$ anions. (N.B., 1 meV \approx 8.066 cm^{-1}).

published structure (e.g., compare the relative agreements between theory and experiment for the $Na_2^{11}B_{10}H_{10}$

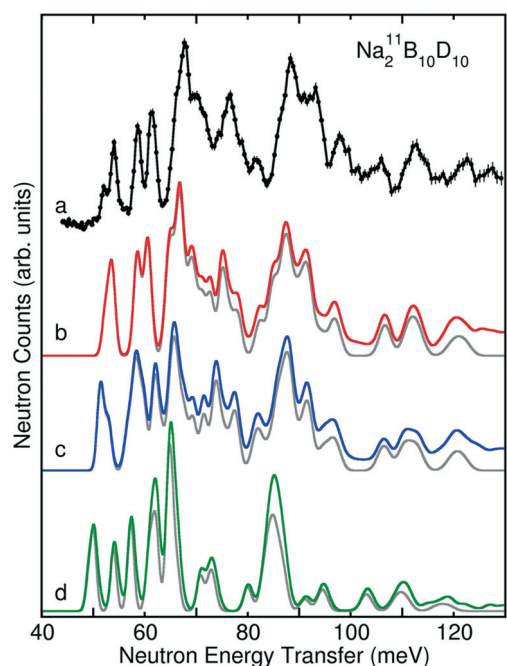


Fig. 9 Neutron vibrational spectrum (a) of $Na_2^{11}B_{10}D_{10}$ at 4 K compared to the simulated one-phonon (gray) and one + two-phonon densities of states (red, blue, and green) from first-principles phonon calculations of the different DFT-optimized structures: (b) current NPD-refined modified structure, (c) published structure,⁹ and (d) "isolated" $^{11}B_{10}D_{10}^{2-}$ anions.

vibrational bands near 57 meV and 120 meV in Fig. 8, which are markedly better for the modified structure). Comparisons of the $\text{Na}_2^{11}\text{B}_{10}\text{D}_{10}$ spectral results in Fig. 9 also reinforce the authenticity of the modified structure and suggest no H-isotope-dependent changes in the monoclinic structural arrangement.

Despite the better spectral agreement for the modified structure, it should be mentioned that the DFT phonon calculations of the energy-optimized version of the published structure indicate no soft phonon modes (*i.e.*, with negative frequencies). This suggests that this version of the structure, similar to that for the modified structure, represents a local minimum on the energy landscape. Yet, we also reiterate that, unlike the modified structure, the published structure changed significantly after energy-optimization, so that the simulated PDOS does not necessarily reflect the original structure. Unfortunately, since generation of the PDOS requires that the optimized structure be at an energy minimum, it is not possible to compute the PDOS of the original “unminimized” structure. In the end, we must heavily weigh the facts that the modified structure (i) fits the NPD data, (ii) results in reasonable Na–H interatomic distances (iii) requires very little energy-optimization, and (iv) leads to a good simulation of the PDOS. Further information about the character, symmetry, and energies of the different phonon modes contributing to the simulated PDOSs of the modified structures of $\text{Na}_2^{11}\text{B}_{10}\text{H}_{10}$ and $\text{Na}_2^{11}\text{B}_{10}\text{D}_{10}$ can be found in Tables S7 and S8 and accompanying animation files in the ESI.†

In closing, this study of $\text{Na}_2\text{B}_{10}\text{H}_{10}$ indicates that structural determinations of these types of complex materials are often nontrivial and require first-principles computations to confirm the stability of any proposed structural model. Moreover, additional spectroscopic validation is highly desirable, especially when multiple energy minima are possible. Such spectroscopic validation may play an especially critical role to corroborate XRPD-derived structures in the absence of complementary NPD data. Our results are leading us to reassess the appropriateness of the previously published monoclinic structures of the heavier $\text{K}_2\text{B}_{10}\text{H}_{10}$ and $\text{Rb}_2\text{B}_{10}\text{H}_{10}$ analogues *via* similar NPD and NVS measurements in combination with DFT computations.

Summary

A new modified monoclinic structure for $\text{Na}_2\text{B}_{10}\text{H}_{10}$ was determined by neutron powder diffraction methods in combination with first-principles computations and neutron vibrational spectroscopy. Compared to the earlier structure,⁹ this modified structure displays identical $P2_1/c$ symmetry but with somewhat different orientations and relatively less distortions of the $\text{B}_{10}\text{H}_{10}^{2-}$ anions. Moreover, it is more stable, displays more reasonable Na–H distances, and results in better overall agreement between calculated and observed neutron vibrational spectra. These results clearly illustrate the utility of both first-principles computations and vibrational

spectroscopy for helping to determine or verify the most physically reasonable crystal structures for a hydrogenous polycrystalline compound from powder diffraction data. This improved $\text{Na}_2\text{B}_{10}\text{H}_{10}$ structure with its theoretical underpinning should enable more accurate modeling of thermodynamic properties for the material, which is important for understanding more completely the dehydrogenation/rehydrogenation cycles associated with NaBH_4 -based hydrogen-storage materials, and for aiding in the design of hybrid $\text{Na}_2\text{B}_{10}\text{H}_{10}$ -based materials with improved Na^+ cation conduction properties for future solid-state Na-ion batteries.

Acknowledgements

This work was partially supported by the US Department of Energy (DOE) Office of Energy Efficiency and Renewable Energy under grant no. DE-EE0002978. Use of the Advanced Photon Source, an Office of Science User Facility operated for the US DOE Office of Science by Argonne National Laboratory, was supported by the US DOE under contract no. DE-AC02-06CH11357. The authors thank Drs. M. R. Hudson and C. M. Brown for their assistance in providing the synchrotron XRPD measurements.

References

- 1 T. J. Udovic, M. Matsuo, W. S. Tang, H. Wu, V. Stavila, A. V. Soloninin, R. V. Skoryunov, O. A. Babanova, A. V. Skripov, J. J. Rush, A. Unemoto, H. Takamura and S. Orimo, *Adv. Mater.*, 2014, **26**, 7622–7626.
- 2 N. Verdal, J.-H. Her, V. Stavila, A. V. Soloninin, O. A. Babanova, A. V. Skripov, T. J. Udovic and J. J. Rush, *J. Solid State Chem.*, 2014, **212**, 81–91.
- 3 A. V. Skripov, O. A. Babanova, A. V. Soloninin, V. Stavila, N. Verdal, T. J. Udovic and J. J. Rush, *J. Phys. Chem. C*, 2013, **117**, 25961–25968.
- 4 T. J. Udovic, M. Matsuo, A. Unemoto, N. Verdal, V. Stavila, A. V. Skripov, J. J. Rush, H. Takamura and S. Orimo, *Chem. Commun.*, 2014, **50**, 3750–3752.
- 5 B. L. Ellis and L. F. Nazar, *Curr. Opin. Solid State Mater. Sci.*, 2012, **16**, 168–177.
- 6 K. B. Hueso, M. Armand and T. Rojo, *Energy Environ. Sci.*, 2013, **6**, 734–749.
- 7 S. Garroni, C. Milanese, D. Pottmaier, G. Mulas, P. Nolis, A. Girella, R. Caputo, D. Olid, F. Teixidor, M. Baricco, A. Marini, S. Suriñach and M. D. Baró, *J. Phys. Chem. C*, 2011, **115**, 16664–16671.
- 8 M. L. Christian and K.-F. Aguey-Zinsou, *ACS Nano*, 2012, **6**, 7739–7751.
- 9 K. Hofmann and B. Albert, *Z. Kristallogr.*, 2005, **220**, 142–146.
- 10 J.-H. Her, W. Zhou, V. Stavila, C. M. Brown and T. J. Udovic, *J. Phys. Chem. C*, 2009, **113**, 11187–11189.
- 11 The mention of all commercial suppliers in this paper is for clarity and does not imply the recommendation or endorsement of these suppliers by NIST.

- 12 E. L. Muetterties, J. H. Balthis, Y. T. Chia, W. H. Knoth and H. C. Miller, *Inorg. Chem.*, 1964, 3, 444–451.
- 13 H. Wu, W. S. Tang, V. Stavila, W. Zhou, J. J. Rush and T. J. Udovic, *J. Phys. Chem. C*, 2015, 119, 6481–6487.
- 14 J. K. Stalick, E. Prince, A. Santoro, I. G. Schroder and J. J. Rush, in *Neutron Scattering in Materials Science II*, ed. D. A. Neumann, T. P. Russell and B. J. Wuensch, Materials Research Soc., Pittsburgh, PA, 1995, pp. 101–106.
- 15 T. J. Udovic, C. M. Brown, J. B. Leão, P. C. Brand, R. D. Jiggotts, R. Zeitoun, T. A. Pierce, I. Peral, J. R. D. Copley, Q. Huang, D. A. Neumann and R. J. Fields, *Nucl. Instrum. Methods Phys. Res., Sect. A*, 2008, 588, 406–413.
- 16 Quantum-ESPRESSO package: www.pwscf.org.
- 17 G. Kresse, J. Furthmuller and J. Hafner, *Europhys. Lett.*, 1995, 32, 729–734.
- 18 T. Yildirim, *Chem. Phys.*, 2000, 261, 205–216.
- 19 K. Momma and F. Izumi, *J. Appl. Crystallogr.*, 2011, 44, 1272–1276.
- 20 H. M. Rietveld, *J. Appl. Crystallogr.*, 1969, 2, 65–71.
- 21 A. C. Larson and R. B. Von Dreele, *General Structure Analysis System*, Report LAUR 86-748, Los Alamos National Laboratory, NM, 1994.
- 22 N. Verdal, W. Zhou, V. Stavila, J.-H. Her, M. Yousufuddin, T. Yildirim and T. J. Udovic, *J. Alloys Compd.*, 2011, 509S, S694–S697.